J. Condensed Matter Nucl. Sci. 15 (2015) 44–54

Research Article

Excess Power during Electrochemical Loading: Materials, Electrochemical Conditions and Techniques

V. Violante*, E. Castagna, S. Lecci, F. Sarto, M. Sansovini, T.D. Makris and A. Torre
ENEA, Unità Tecnica Fusione, C.R. Frascati, Frascati, Italy

D. Knies, D. Kidwell, K. Grabowski and D. Dominguez
Naval Research Laboratory (NRL), Washington, DC, USA

G. Hubler, R. Duncan, A. El Boher and O. Azizi
SKINR, University of Missouri, Columbia, MO, USA

M. McKubre
SRI International Menlo Park, CA, USA

A. La Gatta
Consorzio Veneto Ricerca-TSEM Padova, Italy

Abstract

The critical role of the electrode material characteristics in increasing the probability of observing excess power during electrochemical loading of palladium cathodes with deuterium is investigated, and excess power production obtained using palladium material with these identified characteristics is reported. Characterizations have been performed by using SEM and AFM microscopy as well as electrochemical analysis and XPS. The emerging scenario suggested by these results is that poor control in achieving the identified material status is reflected in the reproducibility of the excess heat phenomenon.

Keywords: Deuterium, Electrolysis, Excess Power, Materials, Palladium

---

*E-mail: vittorio.violante@enea.it

1. Introduction

A significant body of research has been carried out to have a controlled mass transfer of deuterium into palladium cathodes in order to reproducibly exceed the loading threshold [1,2] required to observe excess power production during electrochemical loading [3–6].

The experimental data shows that loading up to about D/Pd = 0.9 (atomic fraction) is a fundamental necessary condition; additional conditions required to observe the onset of the effect [7–9] are enhanced mass transfer, crystal orientation, and specific surface morphology.

Different lots of palladium, most of them from the same producer, gave completely different behavior above the loading threshold D/Pd = 0.9. Three different behaviors have been identified:

(1) Large excess power (>100% of the input power).
(2) Low excess power (<20% of the input power).
(3) No excess power.

The excess heat effect was observed by using also $Pd_{90}Rh_{10}$ cathodes. Some specific features were identified for the active electrodes with both materials. The active palladium electrodes had mostly (100) orientation of the polycrystals, enhanced hydrogen (deuterium) diffusivity, average grain size around 100 microns and a well-defined surface morphology identified by means of the power spectral density function (PSD).

Active $Pd_{90}Rh_{10}$ cathodes have a high diffusivity and a surface morphology, in terms of PSD, very similar to the one belonging to the active Pd samples. The differences are a mixed orientation of the crystals and a lower grain size, typically some ten's of microns. Doping with contaminants has been performed for both Pd and $Pd_{90}Rh_{10}$ cathodes in order to achieve the material characteristics belonging to samples producing excess power.

2. Materials

The most significant evidence related to the cathode behavior in terms of excess power production is the different spectrum of contaminants. It is well known from physical metallurgy that contaminants may have several effects on the metal characteristics:

- Contaminants may act on: grain size, crystal orientation and grain boundaries.

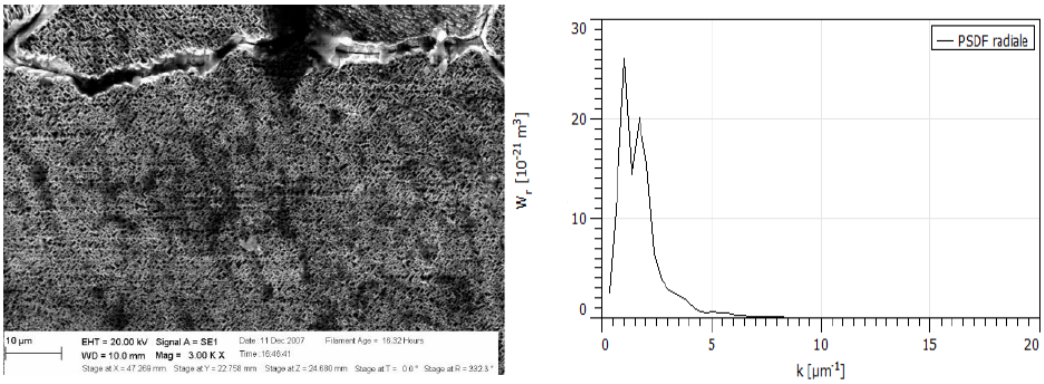

Figure 1. (a, *left*) SEM of the surface of #64 electrode giving up to 3500%. (b, *right*) PSD #64 cathode surface

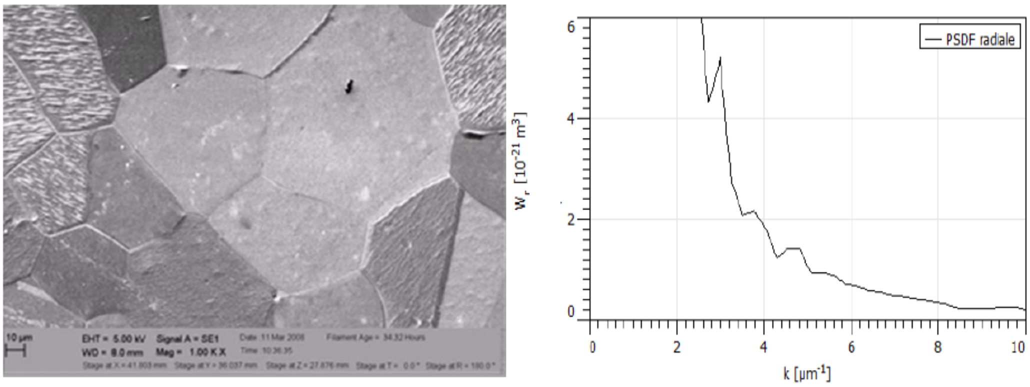

Figure 2. (a, *left*) SEM of a non-active electrode surface. (b, *right*) PSD of non-active electrode surface.

- It is well known from the literature [10] that contaminants modify the effect of chemical etching on surface morphology.

A scanning electron micrograph (SEM) of the surface of #64 cathode that produced up to 3500% excess power reveals what we call a labyrinth morphology as shown in Fig. 1a. This sample displayed the PSD shown in Fig. 1b and we have determined that the PSD and excess power are correlated – they are proportional so the higher the PSD peaks the greater the excess power. By contrast, non-active samples have a very low PSD signal as shown in Fig. 2a,b.

Fabrication of a Pd cathode characterized by crystals mainly (100) oriented, with average grain size around 100 μm and with a surface morphology reproducing a PSD with more than two peaks with decreasing amplitude from the left to the right as in Fig. 1b is not easily achieved. It was understood that materials having a larger concentration of Pt as contaminant gave more often a labyrinth structure such as the one shown in Fig. 1a after the chemical etching with aqua regia. For this reason, two palladium cathodes obtained by using a starting Pd able to give (100) orientation and proper grain size but unable to give the labyrinth structure after etching, were sputtered with a few nanometers of Pt

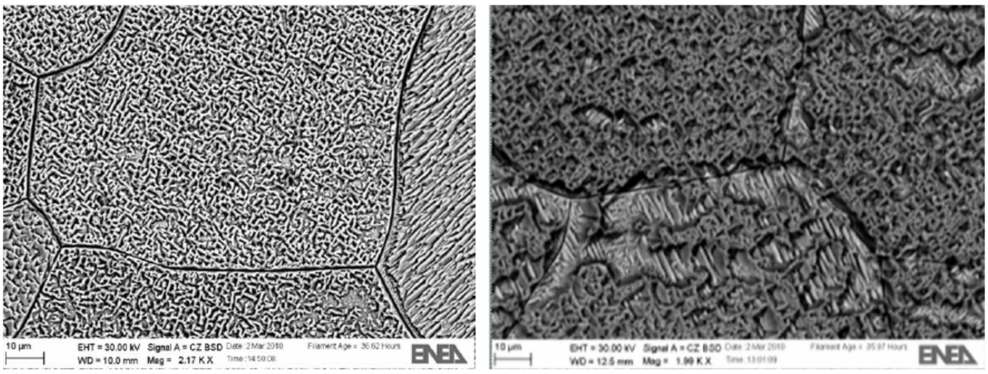

Figure 3. SEM of the surfaces of two Pd samples, doped by adding Pt on the surface and etched with Aqua Regia 50%.

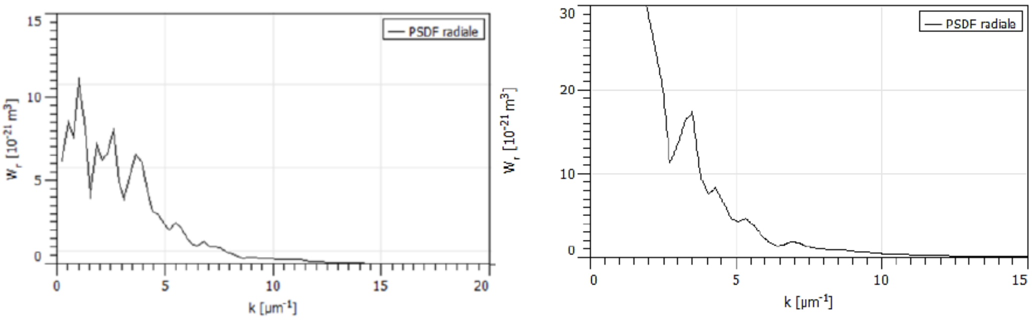

Figure 4. PSD for two Pd samples after Pt deposition, annealing and etching in aqua regia.

and annealed at 850°C. After the thermal treatment the two samples were etched, which produced the required surface morphology as shown in Fig. 3.

The PSD for both the samples were substantially modified compared to the one etched without the deposited Pt (Fig. 2b) as seen in Fig. 4.

These two samples were electrolytically loaded with deuterium in 0.1 M LiOD in two different mass flow calorimeters and both gave excess power up to 25% of the input power. The results are shown in Fig. 5 where power in and power out in milliwatts are plotted versus time in seconds.

A similar study was carried out on $Pd_{90}Rh_{10}$ cathodes prepared by applying the protocol developed at NRL [11]. Palladium and Rhodium have been melted at 90/10 atomic ratios in an alumina crucible by using a hydrogen-oxygen torch. The melted material was annealed at 900 ˚C and then cold rolled to a thickness of 50 μm. After rolling the sample was annealed again at 850°C and then etched with Aqua Regia. Figure 6 shows the surface of sample L119(20–60) after the chemical etching.

A second sample (L119(100–140) was prepared from the produced $Pd_{90}Rh_{10}$ alloy. Both the samples have been analyzed by EDX and we observed some content of Si (Silicon oxide) on the surface of L119(20–60). Figure 7 shows the PSD of the surface of L119(20âĂŞ-60) before electrolysis. We may observe that the PSDF spectral shape is absent. Figure 8 shows the energy dispersive X-ray spectrum (EDX) for sample L119(20–60) where Si is clearly evident.

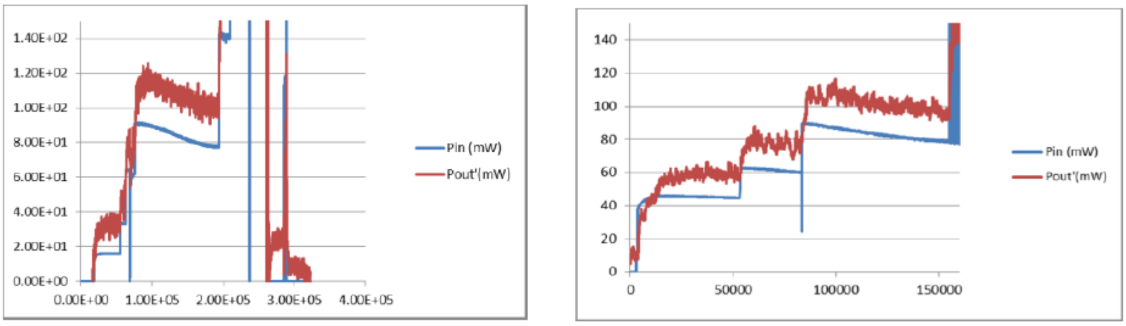

Figure 5. Data showing excess power up to 25% produced by each of the Pd cathodes doped on the surface with Pt before annealing and etching.

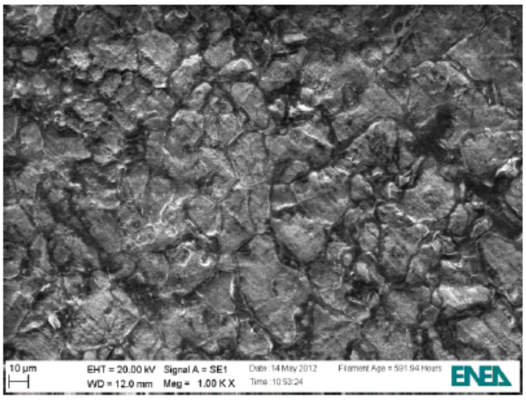

Figure 6. Surface of the L119(20-60) Pd90Rh10 sample.

A calorimetric study on sample L119(20–60) was performed by using the differential calorimeter developed at NRL [12] and the time history of power in and power out is shown in Fig. 9a.

We can observe in Fig. 9a that the excess power spontaneously develops after ∼2,90,000 s elapsed time and was stable for about 12 h. We assumed the effect to be a bias shift of the calorimetric system which was checked by inverting the current to deload the cathode and after deloading an input power level was applied close to the one existing before changing the polarity. After the thermal transient (with some adjusting of the input power at the required level) a perfect balance of power in equals power out was observed (the output curve was overlapping the input curve (see Fig. 9a). This confirmed that the signal was a real effect. The polarity was then reversed again and PdRh was reloaded

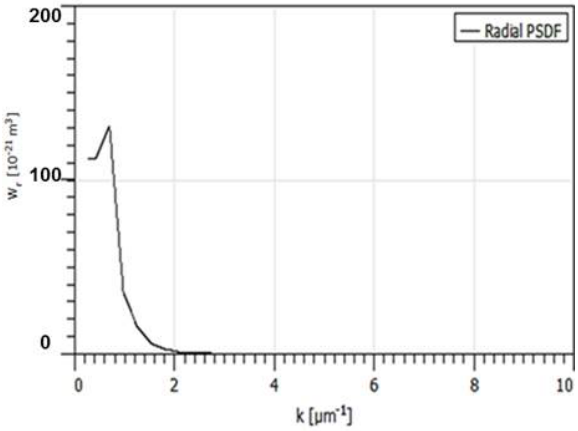

Figure 7. Power spectral density of L119(20-60).

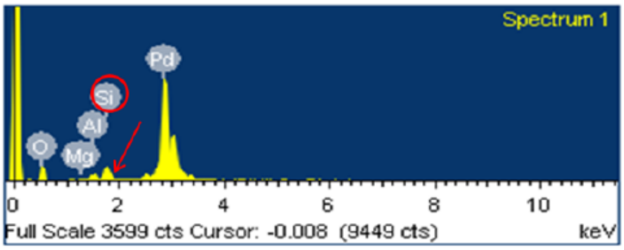

Figure 8. EDX of sample L119(20-60). Si is the most abundant contaminant on the surface.

at a higher current value. As soon as the cathode was reloaded (∼3,55,000 s elapsed time) the system gave again an excess that was larger than the previous one.

Figure 9b shows the same calorimetric run after 5,30,000 s. After ∼5,80,000 s it was decided to perform Galvanostatic Electrochemical Impedance Spectroscopy (GEIS) using the Biologic VP 200 Galvanostat-Potentiostat electrochemical spectrometer that was controlling the experiment. This operation was performed in order to extract, in situ, new information concerning the status of the electrochemical interface in terms of an equivalent circuit.

Five impedance spectra were acquired during the excess but Nyquist plots during the excess gave scattered points, revealing a significant disturbance during the effect; however, one plot was clearly readable after removing the noise. The EIS was carried out within the frequency range 200 kHz–20 Hz and the Nyquist plot is shown in Fig. 10 with frequency decreasing from left to right in the plot. The equivalent circuit during the excess is also shown in the inset in Fig. 10. The Nyquist plot clearly has resonating component inside. The applied DC current during the measurement was 90 mA with 7 mA sine probe amplitude.

The current was then reduced to 30 mA DC and a sufficient time was allowed to elapse (some hours) to complete the thermal transient of the calorimetric equipment (roughly within the time interval 5,90,000—6,50,000 s). The excess power disappeared as can be seen from Fig. 9b and a new impedance analysis was performed and 25 Nyquist plots were acquired within the frequency range 400 kHz–10 Hz. Most of the plots were unstable, yielding very scattered points as during the excess. In some cases it was possible to extract a signal from the noise. Two of them are shown in Figs. 11a,b.

In Fig. 11a the proper fitting of the impedance spectrum was achieved by inserting a typical RLC within the circuit with a resonant frequency of 166 Hz. Figure 11b shows another GEIS plot carried out after switching off the excess and we may see that an equivalent circuit quite similar to the one obtained during the excess power by reducing the current to 30 mA. In this case the equivalent circuit includes LCR components having a resonating frequency of about 200 kHz. After that the current was set to zero for a few seconds and the GEIS was performed again by maintaining the DC current at 30 mA and by applying 3 mA sine wave. The Nyquist plot is shown in Fig. 12. It is clear that RLC component disappeared as soon as input power was set to null.

The surprising result, even if preliminary, is that the excess power is characterized by a specific electrochemical structure of the interface (equivalent circuit) that remains also after switching off the effect by reducing the current, but such a structure is destroyed if the system is more strongly perturbed by reducing the current to zero.

The inductive behavior in Fig. 12 (negative imaginary component) at high frequencies is due to the wiring and connection of the cell and perfectly reproduces the tests performed with dummy circuits.

Even if the results have to be considered as preliminary and need to be replicated, it is clear that the electrochemical interface substantially changes during the production of excess and that the presence of LRC components are suggestive

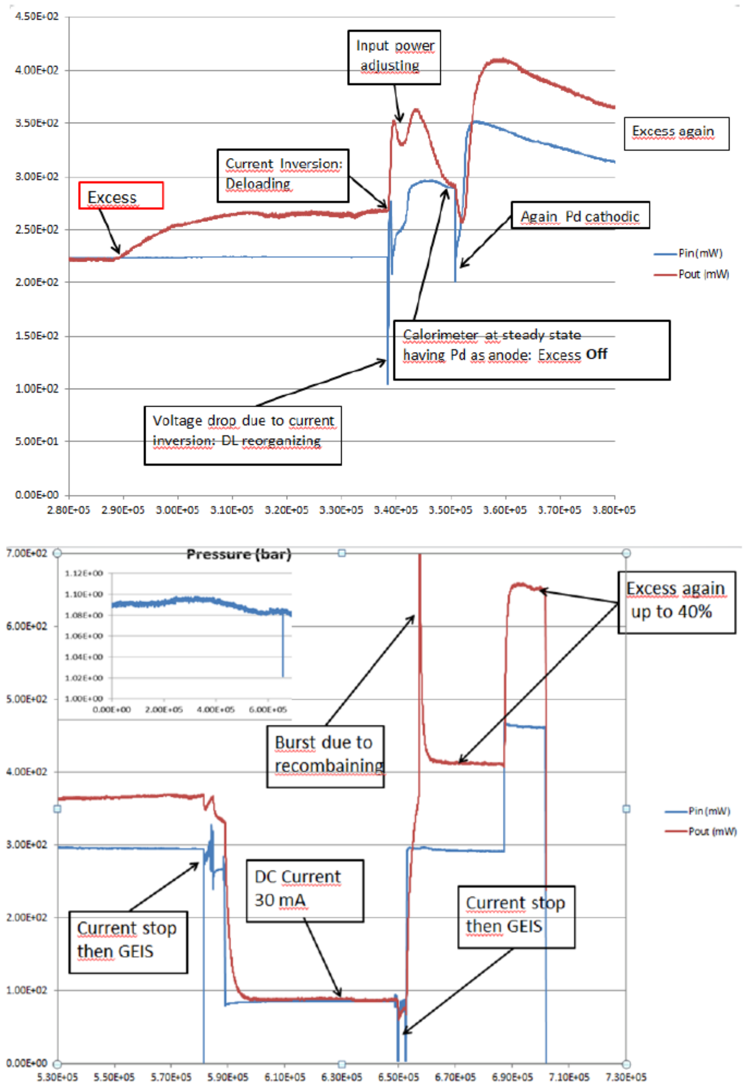

Figure 9. (a, *top*) Excess power occurs (∼2,90,000–3,55,000 s) and is switched off by current inversion. Restoring the original cathodic polarization restarts the power excess. (b, *bottom*) Excess power for the same run as in Fig. 9a at longer time.

of a resonant mechanism at the interface.

By comparison Fig. 13 shows a GEIS at two different current levels performed on an inactive Pd cathode.

As soon as the GEIS was completed, the cell current was increased again to 90 mA and the excess power restarted at a somewhat higher level as can be seen in Fig. 9b. There is a big power spike after increasing the current due to D_2 and O_2 gas recombination as the catalyst restarted as is confirmed by the negative pressure spike in the cell pressure

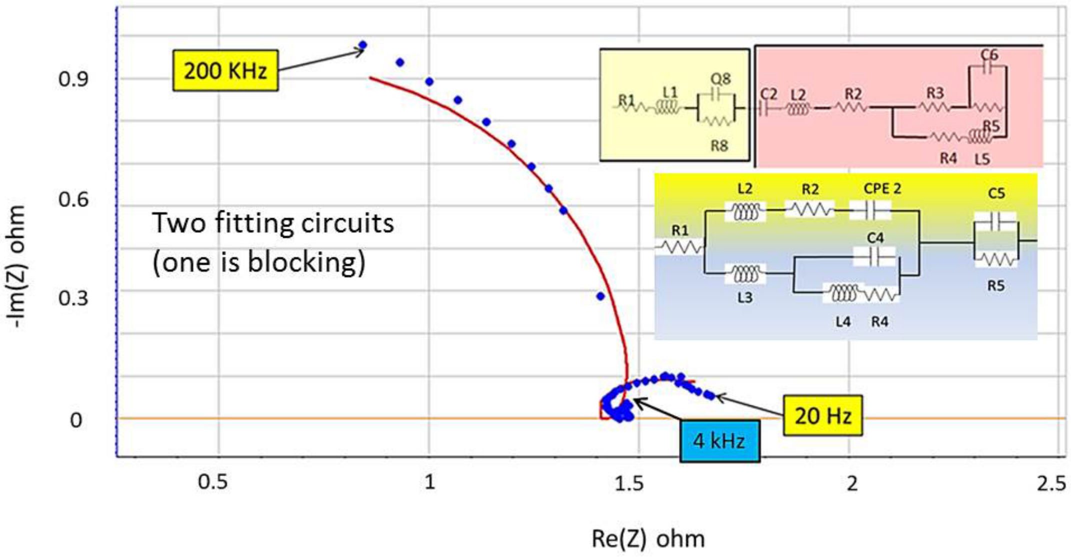

Figure 10. In situ Electrochemical impedance Spectroscopy on Sample L119(20–60). Excess-on.

plot (top left Fig. 9b). Further increasing the current produced greater excess power up to approximately 40% of the input. A small oscillation of both current and potential was observed during the excess.

The cell was switched off during the excess in order to physically investigate the status of the sample surface during an excess power event. Figure 14a shows an SEM image of the electrode surface as it was during the excess. Figure 14b shows the PSD. The most significant peaks are always in the region of k up to about 5 μm^{-1}. EDX revealed that during the excess, Fe, Cu and Pt were on the electrode surface.

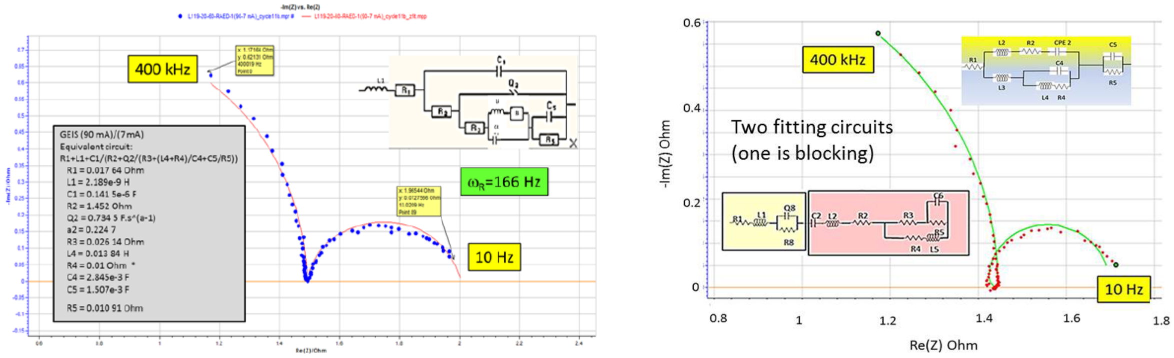

Figure 11. (a, *left*) In situ Electrochemical impedance Spectroscopy on Sample L119(20–60). Excess-off. (b, *right*) In situ Electrochemical Impedance Spectroscopy on Sample L119(20–60). Excess-off.

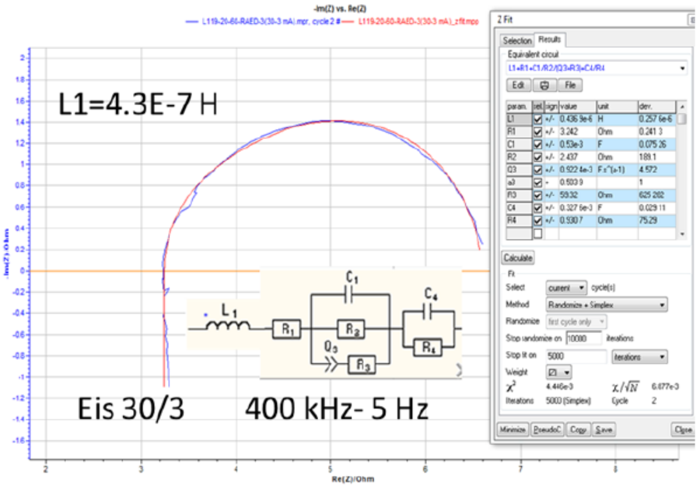

Equivalent circuit: L1+R1+C1/R2/(Q3+R3)+C4/R4

param.	sel.	sign	value	unit	dev.
L1	☑	+/-	0.436 9e-6	H	0.257 6e-6
R1	☑	+/-	3.242	Ohm	0.241 3
C1	☑	+/-	0.53e-3	F	0.075 26
R2	☑	+/-	2.437	Ohm	189.1
Q3	☑	+/-	0.922 4e-3	F.s^(a-1)	4.572
a3	☑	-	0.503 9		1
R3	☑	+/-	59.32	Ohm	625 282
C4	☑	+/-	0.327 6e-3	F	0.029 11
R4	☑	+/-	0.930 7	Ohm	75.29
	☐				

Fit
Select current cycle(s)
Method Randomize + Simplex
Randomize first cycle only
Stop randomize on 10000 iterations
Stop fit on 5000 iterations
Weight ☑
χ^2 4.446e-3 $\chi/\sqrt{N}$ 6.677e-3
Iterations 5000 (Simplex) Cycle 2

Figure 12. GEIS, 30mA/3mA 400 kHz–5 Hz: Excess-Off, anode as reference.

Two additional samples from the sample PdRh lot were investigated and were found to be totally inactive regarding the appearance of excess power.

No evidence of specific surface contaminants was observed on these two samples. Since Si was absent from the surface of the inactive samples, a new lot of PdRh was prepared by intentionally adding Si as a contaminant. One sample was investigated in the differential calorimeter mentioned above.

Figure 15 shows the occurrence of excess power up to 16% with sample L133 (40–80) Si doped. The XPS analysis reveals that Si is in oxide form. The burst continued for 10 h. The large band of the input power before and after the event is due to a superwave current modulation [13]. While we do not have a statistical basis for a conclusion, we may consider that such a result suggests that the presence of specific contaminants on the surface of the electrodes is important to observe excess power.

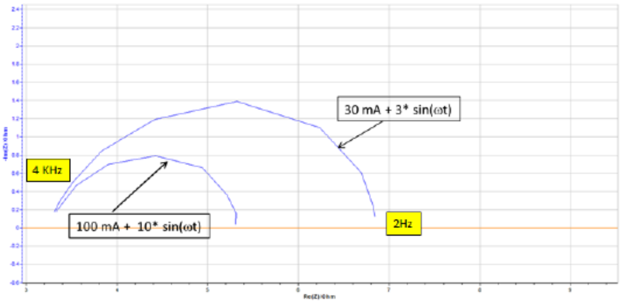

Figure 13. GEIS performed on inactive Pd electrode at two different current levels.

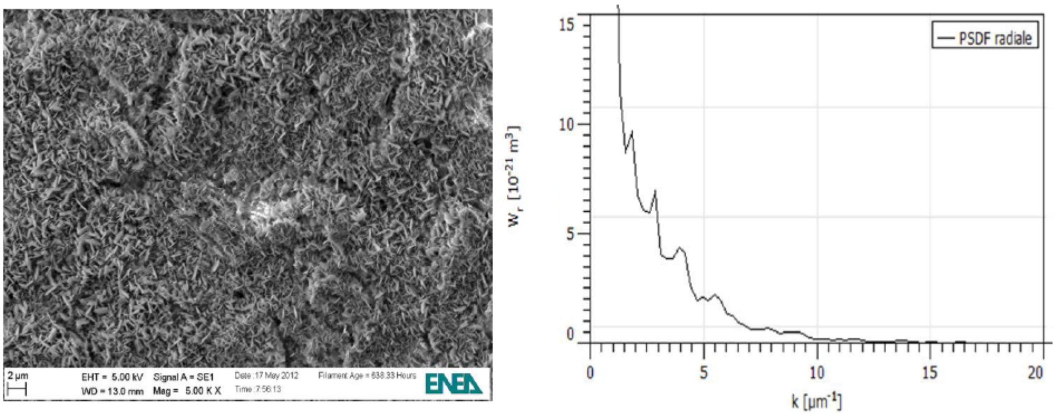

Figure 14. (a, *left*) SEM image of the electrode surface as it was during the production of excess power. (b, *right*) PSD of the surface shown in (a).

3. Conclusions

This paper describes experiments that reveal new information regarding the status of deuterium loaded Pd cathodes during production of excess power in electrolytic cells (0.1 M LiOD, Pt anode, PdRh alloy cathode).

First, electrochemical impedance spectroscopy (EIS) during excess power production reveals the presence of resonances at the surface/electrolyte boundary that requires an LRC component in the circuit diagram to reproduce the Nyquist plot. Second, the LRC component of the Nyquist circuit diagram is still present when the input power is reduced and no excess power is present. Third, the voltage and current during excess power events and after excess power events at reduced input power are unstable causing the EIS to be indecipherable at most times. Forth, as shown previously (reference) there is a strong correlation between the position and strength of peaks in the power spectral density (PSD) of those cathodes that produce excess power. Fifth, though not conclusive, this work suggests that the presence of specific contaminants (Si, perhaps others) on the cathode surface are important for observation of the

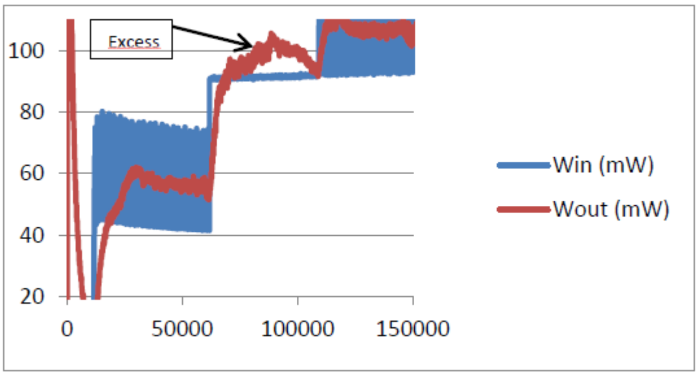

Figure 15. L133 (40–80), Pd90Rh10 Si doped, up to 16% excess power.

excess power. Sixth, this work points to the importance of materials science to achieve the surface morphology, alloy composition, contaminant control and grain orientation [7,8] necessary for the observation of excess power in these material systems.

References

[1] K. Kunimatsu, N. Hasegawa, A. Kubota, N. Imai, M. Ishikawa, H. Akita and Y. Tsuchida, Deuterium loading ratio and excess heat generation during electrolysis of heavy water by a palladium cathode in a closed cell using a partially immersed fuel cell anode, *Proc. Third Int. Conf on Cold Fusion,* Nagoya (Japan), October 20–25, 1992, p. 31.

[2] M.C.H. McKubre, S. Crouch-Baker, A.M. Riley, S. I. Smedly and F. L. Tanzella, Excess power observation in electrochemical stusies of the D/Pd system; the influence of loading, *Proc. Third Int. Conf on Cold Fusion,* Nagoya (Japan), October 20–25, 1992, p. 5.

[3] A. Adrover, V. Violante et al., Stress induced diffusion of hydrogen in metallic membranes, Cylindrical vs. planar formulations I, *J. Alloys and Compounds I* **358**(1) (2003) 268–280.

[4] A. Adrover, V. Violante et al., Stress induced diffusion of hydrogen in metallic membranes, Cylindrical vs. planar formulations II, *J. Alloys and Compounds I* **358**(1) (2003) 157–167.

[5] A. Adrover V. Violante et al., Effects of self-stress on hydrogen diffusion in Pd membranes in the coexistence of α and β phases, *J. Alloys and Compounds* II **368**(1) (2003) 287–297.

[6] V. Violante et al., Consequences of lattice expansive strain gradients on hydrogen loading in palladium, *Phys. Rev. B* **56**(5) (1997) 2417–2420.

[7] V. Violante et al., Material science on Pd–D system to study the occurrence of excess of power, *Proc. ICCF-14*, Washington DC, Vol. 2, 2008, pp. 429–436.

[8] V. Violante et al., Evolution and progressin material science for studying the Fleishmann and Pons effect (FPE), *Proc. ICCF-15*, Oct. 5–9 2009, Rome, Italy, 2009, p. 1.

[9] V. Violante et al., The study of the Fleishmann and Pons effect through the materials science development, *Proc. of the XVI Int. Conf. on Condensed Matter Nuclear Science,* Chennai, India, Feb. 6–11 2011, p. 313.

[10] M.A. Gosàlvez and R.M. Nieminen, *New J. Phys.* **5** (2003) 100.

[11] D.D. Dominguez et al., Are oxides interfaces necessary in Flaischmann and Pons type experiments? *Proc. of the XVI Int. Conf. on Condensed Matter Nuclear Science*. Chennai, India, Feb 6—11, 2011, p. 53.

[12] D. Knies et al., Differential thermal analysis calorimeter at the naval research laboratory, *Proc. ICCF-15,* Oct. 5–9 2009, Rome, Italy, 2009, p. 11.

[13] I. Dardik et al., Intensification of low energy nuclear reactions using superwave excitation, *10th Int. Conf. on Cold Fusion*, Cambridge (MA), USA, 24-29/08/ 2003, p. 61.